



La Science à l'œuvre pour le  
at work for Canada

## NRC Publications Archive Archives des publications du CNRC

### **Performance Evaluation of Three Active Vision Systems Built at the National Research Council of Canada**

Beraldin, Jean-Angelo; El-Hakim, Sabry; Blais, François

#### **NRC Publications Record / Notice d'Archives des publications de CNRC:**

<http://nparc.cisti-icist.nrc-cnrc.gc.ca/npsi/ctrl?action=rtdoc&an=8913603&lang=en>

<http://nparc.cisti-icist.nrc-cnrc.gc.ca/npsi/ctrl?action=rtdoc&an=8913603&lang=fr>

Access and use of this website and the material on it are subject to the Terms and Conditions set forth at

[http://nparc.cisti-icist.nrc-cnrc.gc.ca/npsi/jsp/nparc\\_cp.jsp?lang=en](http://nparc.cisti-icist.nrc-cnrc.gc.ca/npsi/jsp/nparc_cp.jsp?lang=en)

READ THESE TERMS AND CONDITIONS CAREFULLY BEFORE USING THIS WEBSITE.

L'accès à ce site Web et l'utilisation de son contenu sont assujettis aux conditions présentées dans le site

[http://nparc.cisti-icist.nrc-cnrc.gc.ca/npsi/jsp/nparc\\_cp.jsp?lang=fr](http://nparc.cisti-icist.nrc-cnrc.gc.ca/npsi/jsp/nparc_cp.jsp?lang=fr)

LISEZ CES CONDITIONS ATTENTIVEMENT AVANT D'UTILISER CE SITE WEB.

Contact us / Contactez nous: [nparc.cisti@nrc-cnrc.gc.ca](mailto:nparc.cisti@nrc-cnrc.gc.ca).



National Research  
Council Canada

Conseil national  
de recherches Canada

Canada

**PERFORMANCE EVALUATION OF THREE ACTIVE VISION SYSTEMS  
BUILT AT THE NATIONAL RESEARCH COUNCIL OF CANADA**

Optical 3-D Measurement Techniques III

Vienna, Oct. 2-4, 1995, pp.352-361

NRC 39165

**J.-A. Beraldin, S. F. El-Hakim, and F. Blais**

Institute for Information Technology

National Research Council of Canada

Ottawa, Ontario, Canada K1A 0R6

**ABSTRACT**

Active 3-D vision systems, such as laser scanners and structured light systems, obtain the object coordinates from external information such as scanning angles, time of flight, or shape of projected patterns. Passive systems require well-defined features such as targets and edges and are affected by ambient light. Therefore, they have difficulty with sculptured surfaces and unstructured environments. Active systems provide their own illumination so they can easily measure surfaces in most environments. However, their accuracy drops when measurements are performed on objects with sharp discontinuities such as edges, holes, and targets. In most applications, measurements on both surfaces and on these types of features are all required to completely describe an object. This means that systems based on only range or intensity will not provide sufficient data for these applications. The integration of range and intensity data to improve vision-based three-dimensional measurement is therefore required. In addition, a user must contend with the fact that the accuracy obtained from the various types of vision systems, as a function of the viewing volume, have significantly different behaviours. Therefore, each type of sensor is more suited for a specific type of object or scene. The techniques described in this paper to measure the test scenes integrate the registered range and intensity data produced by these range cameras with the objective to provide highly accurate dimensional measurements. The range cameras, the calibration procedures, and results of measurements on test objects are presented in the paper.

## 1. INTRODUCTION

### 1.1. Measurement of Object Features

The type of feature being measured is an important factor affecting the accuracy of a machine vision system. Therefore, selecting a vision system for a particular application must take into account the ability of the system to measure the features of interest with the required accuracy. In a large number of applications, where vision systems are considered, different types of features are required to fully represent an object. In the processing steps, an object is represented by geometric entities<sup>1</sup>: vertices (points), boundaries (edges), and surfaces. In addition, topological parameters, or the relationships between these entities, are also part of the object representation. In some objects, such as polyhedron types and simple sheet metals, vertices and edges may be sufficient. However, many other manufactured objects will also require curved and free form surfaces to be measured. The capabilities of a vision system to extract and to measure accurately these different types of primitives vary from one technology to another. In addition, many applications do not allow any alterations to the object to suite the vision system, e.g., by placing markings or changing the reflectivity of the surface. Hence, non-contact vision systems are preferred for these applications.

### 1.2. Previous Work

Among the many non-contact techniques proposed to extract 3-D information from a scene, active triangulation is used in applications as diverse as reverse engineering<sup>2</sup> and wood measurement<sup>3</sup>. Three digital 3-D imaging systems based on two different optical arrangements were developed and demonstrated at the National Research Council of Canada (NRC). They are the auto-synchronized principle<sup>4</sup> and the BIRIS system<sup>3</sup>. These range cameras provide registered range and intensity data for visible surfaces. However, like many active range cameras, they have difficulty with features like edges, holes, and targets. Some systems based upon mirror-like optical arrangements (BIRIS) or dual-detector arrangements are capable of eliminating some of the problems. The registered intensity image generated by a range camera can be used advantageously to alleviate the impact of erroneous range on edge measurements<sup>5</sup>. The range image is used to determine the shape of the object (surfaces) while the intensity image is used to extract edges and features such as holes and targets.

For active range cameras, accuracy evaluation has been investigated, albeit less extensively than in 2-D systems.<sup>1,5-8</sup> Comparison of the measurement accuracy of various range vision technologies, based on the same tests and criteria, are difficult to find in the literature. Therefore, the objective of this paper is to provide accuracy figures on a variety of test objects in order to fill some of the gap found in the literature and to encourage vision system

manufacturers and users to publish accuracy results with similar testing procedures. In the next section, the characteristics of the three range cameras are summarized. A special facility for calibration and evaluation of vision systems and techniques will be described in section 3. Sample results will be given in section 4 to provide accuracy numbers for different types of features using the three range cameras. Concluding remarks appear in Section 5.

## 2. CHARACTERISTICS OF NRC 3-D VISION TECHNOLOGIES

### 2.1. Auto-synchronized Scanner Approach

Rioux<sup>4</sup> introduced a synchronized scanning scheme, with which large fields of view with small triangulation angles can be obtained without sacrificing precision. With smaller triangulation angles, a reduction of shadow effects is inherently achieved. The intent is to synchronize the projection of the laser spot with its detection. With this optical setup, the instantaneous field of view of the position detector follows the spot as it scans the scene. Therefore, the focal length of the lens is related to the desired depth of field (DOF) and not to the field of view (FOV). Implementation of this triangulation technique by an auto-synchronized scanner approach allows a considerable reduction in the optical head size compared to conventional triangulation methods. Figure 1 depicts the auto-synchronization effect produced by a double-sided mirror (see X-Axis Scanner).

### 2.2. Generation of Surface Maps

A 3-D surface map can be captured in three ways. The triangulation plane defined by the laser beam can be

- 1- translated in a direction orthogonal to it with a precise translation stage,
- 2- rotated around an axis parallel to it with a precise rotation stage,
- 3- or, scanned by a second mirror that is placed orthogonal to the first one.

By translating or rotating the object, one can achieve similar results.

Figure 1 displays schematically the basic components of a dual scan axis auto-synchronized camera (option 3). See Beraldin *et al.*<sup>7</sup> for the functions of 3-D coordinate's computation. The camera that uses this third option is known as the Random Access Laser (**RAL**) scanner. The other range camera based upon the auto-synchronized scanner approach uses option 1. It is known as the **Colour** Scanner because this camera uses a laser source composed of three wavelengths (Red, Green, Blue) to acquire colour along with shape.

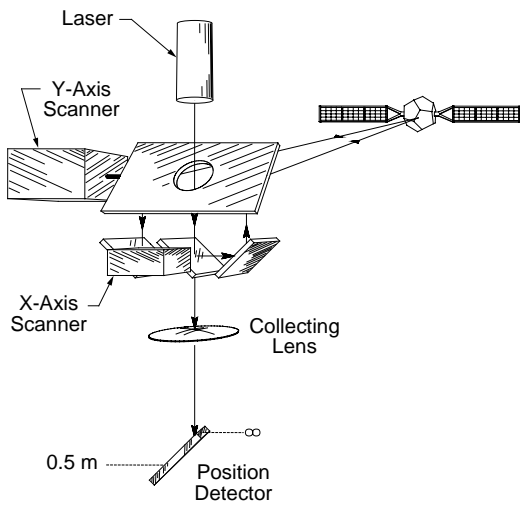


Figure 1: Auto-synchronized scanner.

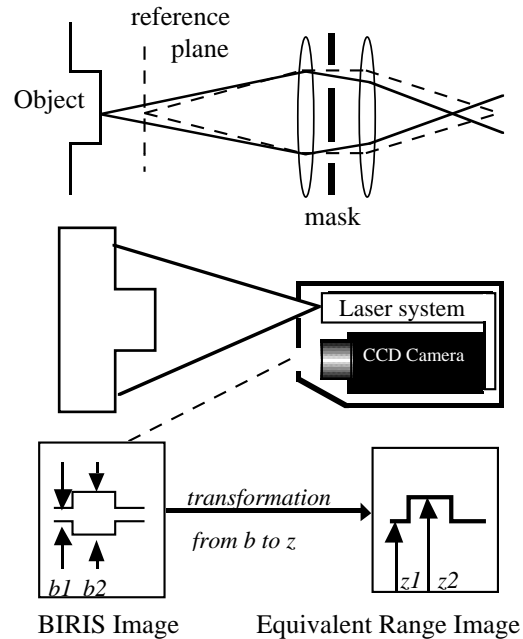


Figure 2: The BIRIS range sensor

### 2.3. BIRIS Technology

The BIRIS range sensor was developed to work in difficult environments where reliability, robustness, and ease of maintenance are as important as the accuracy. Hence, these choices were made at the expense of a reduced accuracy, i.e., two to three compared to the other scanners (shown later in the results). The optical principle of BIRIS is shown in Figure 2. The main components are a mask with two apertures, a camera lens, and a standard CCD camera. In a practical implementation, the double aperture mask replaces the iris of a standard camera lens (hence the name bi-iris). A laser line, produced by a solid-state laser diode and a cylindrical lens, is projected on the object and a double image of the line is measured on the CCD camera. The separation between the two imaged lines is proportional to the distance between the object and the camera. Hence, it provides direct information about the shape and dimensions of the object. For example, in Figure 2, the line's separation  $b_1$  and  $b_2$  represent the ranges  $Z_1$  and  $Z_2$  respectively.<sup>3</sup>

### 2.4. Calibration Procedures

Owing to the shape of the coordinate system spanned by the variables measured with range cameras, the resultant images are not compatible with the coordinate systems used by most geometric image processing algorithms, e.g., rectangular coordinate system. A calibration of the range camera is therefore required for any scanning method. The calibration techniques used at NRC can be divided in two groups<sup>7</sup>: table look-up construction with linear

interpolation or local model fitting and global model fitting. The expected precision for all three range cameras is shown in figure 3. These curves are computed from the error propagation of measurements of the position of the laser spot on the detector, the scanning mirror or motion stage controller, and the geometry of the sensor. Table 1 provides some of the specifications of the three range cameras.

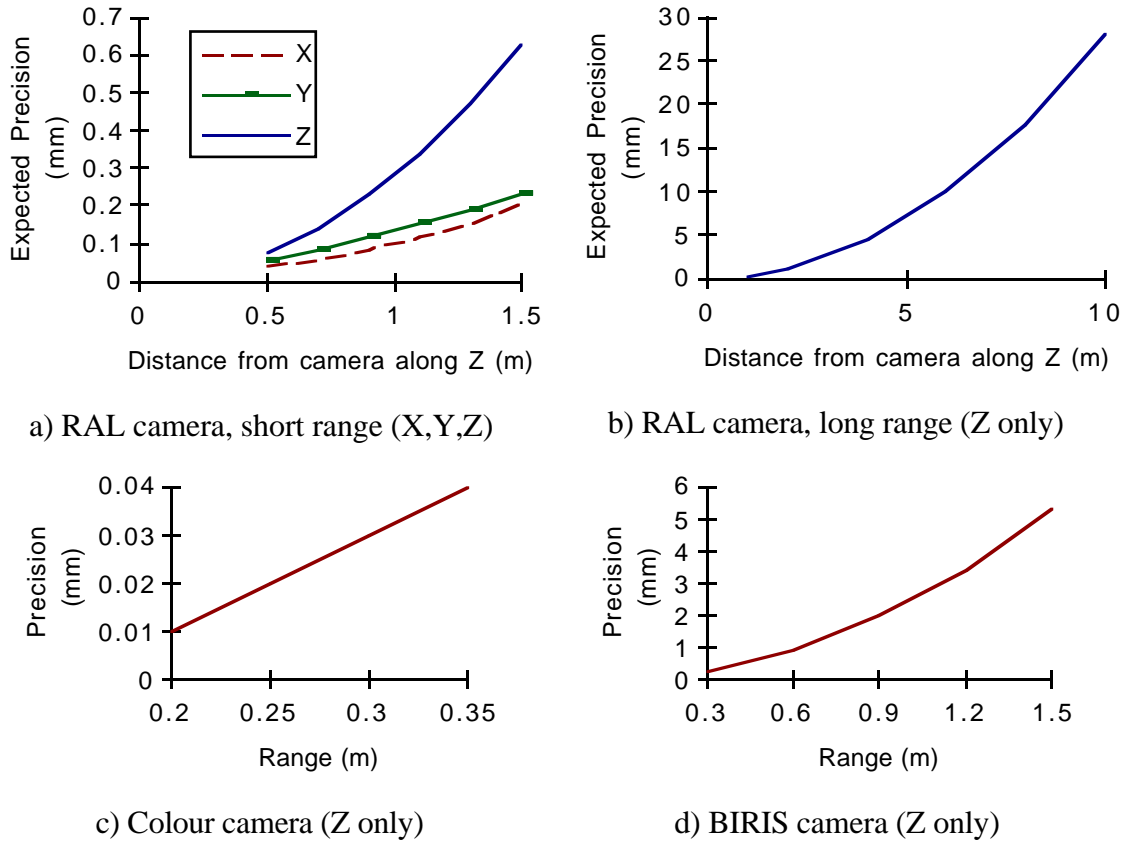


Figure 3: Expected precision of the range cameras.

Table 1. Range cameras Specifications

Specification	RAL Camera	Colour Camera	BIRIS
FOV	30° x 40°	40°	30°
Standoff	0.5 m	0.2 m	0.3 m
DOV	0.5 m and up	0.10 m	2.0 m
Image Resolution X,Y	up to 4096 x 4096	up to 4096	up to 512
Z precision	see curve	see curve	see curve
Data Rate	20 kHz	20 kHz	15.75 kHz

### 3. THE CALIBRATION AND EVALUATION LABORATORY - CEL

A laboratory at the Institute for Information Technology of the NRC has been dedicated to calibration and evaluation of machine vision sensors and systems. Specifically, the objectives of CEL are 1) to perform precise calibration of various types of sensors and systems, 2) to

monitor sensor stability over time and under variations in environmental conditions such as temperature and ambient light, 3) to evaluate system geometric measurement accuracy on a wide range of specially designed standard objects and high-precision positioning devices, and, 4) to validate computer vision algorithms, such as target and edge measurement, multi-view registration, model-based recognition, and sensor fusion.

The laboratory (figure 4) is currently equipped with: precise targets in various arrangements, optical bench (with vibration isolators), high precision translation and rotation stages, theodolites and electronic distance measurement devices, standard test objects, PC and SGI workstations. Software tools include, among others: calibration (including added distortion parameters), measurement and inspection using 3-D data produced by various types of vision systems, display and manipulation of 3-D data files, statistical analysis packages.

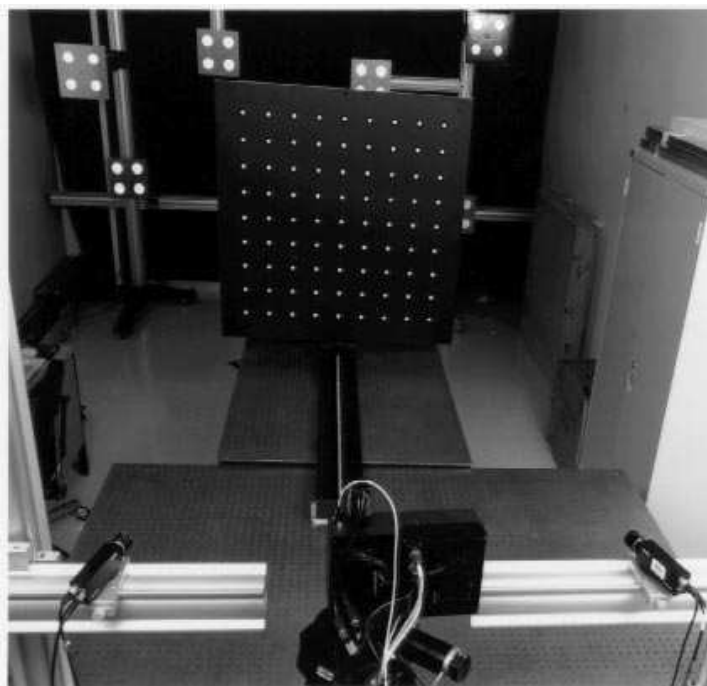


Figure 4: Part of CEL showing camera mounts, translation stage and targets.

## 4. TEST PROCEDURE AND RESULTS

### 4.1. Standards for Performance Tests

Our criterion for comparing 3-D technologies is based on how accurately the object or the site is recovered. The accuracy (defined below) is expressed relative to the field of view (FOV). This is the most critical factor that limits the use of a sensor and usually is not explicitly provided by manufacturers. The other criteria for evaluation, such as speed, depth of field (DOF), and costs are also important, however, the way they influence the selection criteria is an engineering issue that is beyond the scope of this paper.

ANSI standard for automated vision systems-performance test-measurement of relative position of target features in two dimensional scenes<sup>9</sup>, is followed here, with changes to suit the 3-D space. The following two definitions, taken from those standards, will be used in this paper:

**Accuracy:** The degree of conformance between a measurement of an observable quantity and a recognized standard or specification that indicates the true value of the quantity.

**Repeatability (precision):** The degree to which repeated measurements of the same quantity varies about their mean.

We now add one other test procedure:

- For object surfaces and 3-D edges, the accuracy is calculated by comparing the given parameters of the surface or edge-curve function to the computed parameters from fitting the measured data to the function. The various test objects are shown in figure 5.

Objects A, B, C and D have known surface parameters while object E, which will be used for edge-measurement tests, has various circular holes of known sizes. For all range cameras, extensive repeatability tests, over several days and at varied temperatures, showed that the data produced are stable at the noise level of the sensor and that the calibration is valid over time. All the objects were measured with a coordinate measuring machine (CMM) with an accuracy

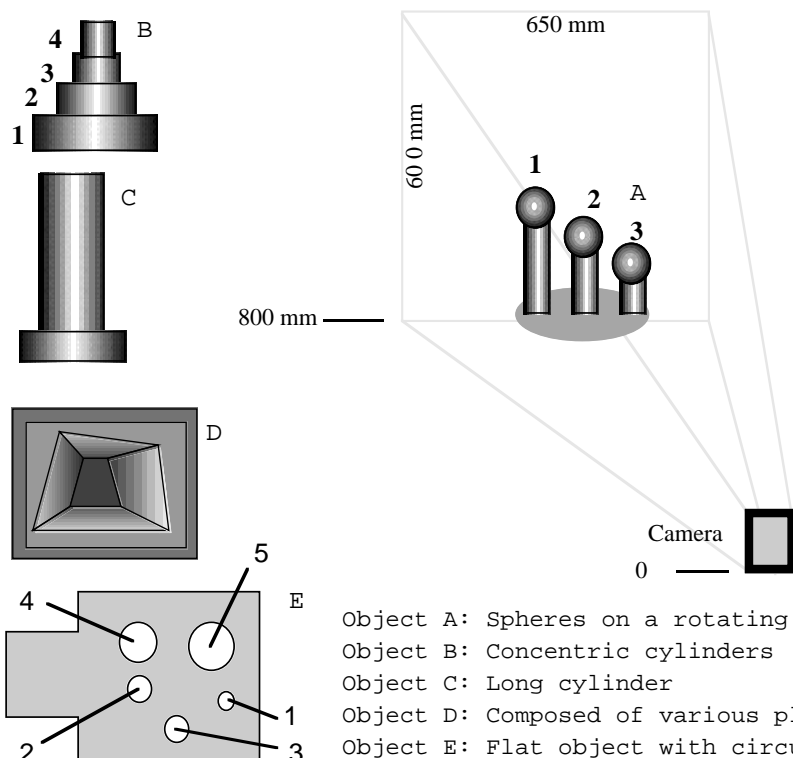


Figure 5: Camera set up for evaluation tests and test objects. better than 0.005 mm. The precision reported in fig. 3 are well above that value, thus, the CMM measurements are within the standards. Because of the limited number of pages, most of the results are given for the **RAL** scanner. For this scanner, the field of view (FOV) used for the reported tests is about 650 mm by 600 mm when the objects are placed at about 800 mm from the camera.

#### 4.2. Test Results on Surfaces

Table 2 shows a sample of the results on object A with the **RAL** scanner. The object, mounted on a rotating table, was scanned at numerous angular positions. At every position, the X, Y, and Z coordinates of each surface were segmented from the background using a

region growing technique. A sphere was fitted on the data and the radius ( $R$ ) along with the center ( $X_c, Y_c, Z_c$ ) of the sphere were determined. The mean at each position and the standard deviation of the repeated measurements are given for sphere #1 only. Tables 3 and 4 show results of measurements on cylinders (objects B and C) with the **RAL** camera. Surface orientation is another issue that can be examined. One might wonder how well angles between planes can be determined.

Table 2: Results on spheres for RAL scanner.

Measurement	Sphere 1			
	R	$X_c$	$Y_c$	$Z_c$
<b>Rotation: <math>0^\circ</math></b>				
Mean	28.61	187.17	-25.82	555.49
$\sigma$	0.09	0.02	0.01	0.10
<b>Rotation: <math>90^\circ</math></b> computed = $89.945^\circ$ error = $-0.055^\circ$				
Mean	28.31	186.16	123.14	605.51
$\sigma$	0.06	0.02	0.02	0.06
<b>Rotation: <math>135^\circ</math></b> computed = $134.685^\circ$ error = $-0.315^\circ$				
Mean	28.20	185.60	128.72	690.43
$\sigma$	0.07	0.04	0.01	0.08
<b>Rotation: <math>-45^\circ</math></b> computed = $-44.934^\circ$ error = $-0.066^\circ$				
Mean	28.19	187.09	-81.84	619.37
$\sigma$	0.11	0.12	0.02	0.12
$\sigma$ -mean	0.07	0.04	0.01	0.08
R-true	28.29			
R-bias	RMS: 0.22 mm Max.: 0.40 mm			

An object with 10 planar surfaces was manufactured from a stable material and with tight tolerances and measured with the same CMM (object **D**). It measures about 200 mm by 200 mm by 100 mm.

Table 3: Sample results on cylinders (bias) for RAL scanner.

Measurement	Cyl. B-1	Cyl. B-2	Cyl. B-3	Cyl. B-4	Cyl. C
Radius - mm	39.39	29.81	22.45	12.75	44.25
Axis Angle $^\circ$	88.41	88.41	88.49	88.39	89.60
True Radius	39.63	30.02	22.60	12.75	44.42
Radius Bias	-0.24	-0.21	-0.15	0.00	-0.17

Table 4: Sample results of repeatability test on cylinder B-2

Measurement	# 1	# 2	# 3	# 4	# 5	Mean	$\sigma$
Radius - mm	29.86	29.79	29.80	29.83	29.79	29.81	0.03
Axis Angle $^\circ$	88.54	88.35	88.51	88.43	88.24	88.41	0.11

Table 5: Angle between planes: **RAL**

Plane	Surface angle	fit-residual RMS	angle residual $^\circ$
Plane 1	0	0.139	0.0
Plane 2	0	0.132	0.425
Plane 3	20	0.121	-0.273
Plane 4	30	0.132	0.124
Plane 5	40	0.112	-0.476
Plane 6	10	0.128	0.090
all planes	fitting-plane RMS : 0.127 mm surface angle RMS: 0.290 deg.		

Table 6: Angle between planes: **Colour**

Plane	Surface angle	fit-residual RMS	angle residual $^\circ$
Plane 1	0	0.012	0.0
Plane 2	0	0.026	0.028
Plane 3	20	0.027	-0.222
Plane 4	30	0.021	-0.190
Plane 5	40	0.033	0.248
Plane 6	10	0.016	-0.040
all planes	fitting-plane RMS : 0.023 mm surface angle RMS: 0.169 deg.		

Table 5 gives the results (referenced to plane #1) obtained with the **RAL** camera and Table 6 for the **Colour** camera. From all the tests on surfaces, the accuracy of the **RAL** camera, on unmarked surfaces and over a range up to 2.5 m, is about 1:3500 relative to the FOV, for the **Colour** scanner about 1:6500, and, for BIRIS the accuracy is about 1:2500 when similar tests are applied.

### 4.3. Test Results on Targets

The target plate mounted on a translation stage (figure 4) was scanned by the **RAL** camera at various ranges between 500 mm and 2500 mm. For larger distances, retro-reflective targets mounted on a stable frame at various ranges (shown in figure 4 on the back wall) were used. The true positions of the targets on the plate were measured with the same CMM while those of the targets on the far frame were measured with a theodolite. The distances between all the targets were computed and compared to the true distances. Table 7 shows the RMS values of the differences at sample distances using the **RAL** camera.

Table 7: Sample Results of target measurements at various distances (mm)

Distance (mm)	FOV (mm <sup>2</sup> )	RMS-X	RMS-Y	RMS-Z	accuracy-XY	accuracy-Z
800	650 x 600	0.080	0.102	0.155	1 : 7200	1 : 4200
2200	1750 x 1500	0.226	0.235	0.672	1 : 7600	1 : 2600
5600	4500 x 4100	0.611	0.539	1.950	1 : 7700	1 : 2300

### 4.4. Test Results on Edges

The flat metal object E contains circular edges of known radii (fig. 5). The object was scanned at various orientations using the rotating table. The edges were extracted from the intensity image produced by the sensor, using a morphologic edge detection technique. Edge points were then extracted with sub-pixel accuracy and the corresponding X, Y, and Z coordinates were obtained from the 3-D image. A 3-D planar circle is fitted to each group of 3-D coordinates of edge points and the radius and center coordinates were computed. Table 8 shows sample results using the **RAL** camera.

Table 8: Edge measurements of circles

Circle #	True Rad.	Radius	Error (mm)
<b>Rotation: 0°</b>			
1	10.000	9.900	- 0.100
2	12.482	12.342	- 0.140
3	14.990	15.150	+0.160
4	19.998	20.048	+0.050
5	24.987	24.891	- 0.096
<b>Rotation: 10°</b>			
1	10.000	9.901	- 0.099
2	12.482	12.336	- 0.146
3	14.990	15.144	+0.154
4	19.998	20.002	+0.004
5	24.987	24.887	- 0.100
<b>Rotation: 20°</b>			
1	10.000	9.918	- 0.082
2	12.482	12.546	+0.064
3	14.990	15.095	+0.105
4	19.998	19.925	- 0.073
5	24.987	25.016	+0.029
<b>Rotation: 30°</b>			
1	10.000	9.802	- 0.198
2	12.482	12.897	+0.415
3	14.990	14.768	- 0.222
4	19.998	19.860	- 0.138
5	24.987	25.199	+0.212

For the **RAL** scanner, the accuracy on edges obtained from all the tests translates to about 1:7500 of the FOV. For the **Colour** and **BIRIS** cameras, similar tests were performed and the resulting accuracy was about 1:3500 and 1:1500 respectively.

## 5. CONCLUDING REMARKS

An approach to evaluating the measurement accuracy of range cameras has been presented. The procedure can be applied to passive and active systems. A specially equipped calibration and evaluation laboratory has been used to evaluate the 3-D vision systems developed at the NRC. They demonstrate that it is possible to achieve accuracy figures that are at about the same level as the measured precision of a vision system as long as the calibration is stable. Auto-synchronized systems can provide a complete 3-D map of surfaces, edges and targets, with better than 1:3500 accuracy while for the **BIRIS** system, it is at about 1:2000. Selection of a range camera is largely dependent on the type of feature to be measured and the required accuracy. Further investigation will include the determination (theoretically and experimentally) of the variance-covariance matrix of the spatial error distribution and the certification of the test objects.

## 6. REFERENCES

1. S.F. El-Hakim, J.-A. Beraldin and F. Blais, "A Comparative Evaluation of Passive and Active 3-D Vision Systems", *Proc. Dig. Photogram.*, St-Petersburg, June 25-30, 1995.
2. P. Boulanger, "Reverse Engineering of Complex Surfaces based on a New Hierarchical Segmentation Method," *Videometrics II*, SPIE-2067, 186-197, 1993.
3. F. Blais, M. Lecavalier, J. Domey, P. Boulanger and J. Courteau, "Application of the BIRIS Range Sensor for Wood Volume Measurement," NRC-ERB-1038, October, 92.
4. M. Rioux, "Laser Range Finder based on Synchronized Scanners," *Appl. Opt.*, 23, 3837-3844, 1984.
5. S.F. El-Hakim and J.-A. Beraldin, "On the Integration of Range and Intensity Data to Improve Vision-based Three-dimensional Measurements", *Videometrics III*, Proc. SPIE 2350, 306-321, 1994.
6. P.J. Besl, "Active, optical range imaging sensors", *MachineVision and Applications*, 1(2), 127-152, 1988.
7. J.-A. Beraldin, S.F. El-Hakim and L. Cournoyer, "Practical Range Camera Calibration", *Videometrics II*, SPIE-2067, 21-31, 1993.
8. J. Paakkari and I. Moring, "Method for evaluating the performance of range imaging devices", *Proc. Industrial Applications of Optical Inspection, Metrology, and Sensing*, SPIE-1821, 350-356, 1992.
9. *American National Standard for Automated Vision Systems - Performance Test - Measurement of Relative Position of Target Features in Two-Dimensional Space*. ANSI/AVA A15.05/1 - 1989.